JOURNAL OF CATALYSIS **103**, 450–465 (1987)

Carbon-Supported Fe–Mn and K–Fe–Mn Clusters for the Synthesis of C_2–C_4 Olefins from CO and H_2

I. Chemisorption and Catalytic Behavior

JEREMY VENTER,* MARK KAMINSKY,† GREGORY L. GEOFFROY,†
AND M. ALBERT VANNICE*,[1]

*Department of Chemical Engineering and †Department of Chemistry, The Pennsylvania State University,
University Park, Pennsylvania 16802

Received January 8, 1986; revised October 1, 1986

Highly dispersed Fe–Mn bimetallic particles were obtained on a high-surface-area amorphous carbon black support using Fe–Mn and K–Fe–Mn carbonyl clusters. These catalysts were characterized by hydrogen adsorption and by CO chemisorption at 195 and 300 K, and their kinetic behavior for CO hydrogenation was studied at 1 atm in a differential, plug-flow microreactor. The K-promoted clusters with stoichiometries of KMnFe and $KMnFe_2$ gave 85–90 wt% ethylene, propylene, and butene with methane as the only other detectable hydrocarbon product. The KFe_3 cluster also had a high selectivity to olefins but showed somewhat more chain growth. The nonpromoted Mn–Fe catalysts with Fe/Mn = 2, prepared from either stoichiometric mixed-metal carbonyl clusters or coimpregnation of the separate Fe and Mn carbonyl clusters, also had a high selectivity to light olefins; however, this selectivity was strongly dependent upon the pretreatment. The properties of the FeMn clusters without K is consistent with a proposed model in which a surface spinel, $(Fe_{1-y}Mn_y)_3O_4$, plays a principal role in providing high selectivity to light olefins.

INTRODUCTION

An important aspect of Fischer–Tropsch chemistry is the development of catalysts for selectively producing olefinic feedstocks for the chemical industry (1). Schulze showed that the selective production of short-chain olefins from coal can be competitive to olefins derived from oil (*2*), and the development of catalysts with higher yields of lower molecular weight olefins has made progress. These catalysts, all of which contain iron, can be divided into six groups (*3, 4*):

(1) Well-known K-promoted Fe catalysts (*5–7*).
(2) Iron catalysts modified by addition of Co or the oxides of Ti, V, Mo, and Mn (*8, 9*).
(3) Partially sulfur-poisoned catalysts (*10–13*).
(4) Proprietary iron-based catalysts developed by SASOL Co. (*3*).
(5) Alloy and coprecipitated manganese catalysts developed by Kölbel containing 10–20 wt% iron (*14, 15*).
(6) Carbon-supported catalysts (*16, 17*).

Introduction of manganese into bulk Mn/Fe Fischer–Tropsch catalysts prepared by coprecipitation or alloying is known to increase the olefin selectivity (*12, 18–34*). In addition, various organometallic compounds [$Fe(CO)_5$, $Fe(AcAc)_2$, and $Fe(AcAc)_3$] were used by Barrault and co-workers to prepare catalysts of Fe supported on MnO and MnO_2 (*35–37*). Bruce, Hope, and Turney studied $NEt_4[Fe_2Mn(CO)_{13}]/SiO_2$, $K[Fe_2Mn(CO)_{13}]/SiO_2$ and nitrate-derived catalysts (*38*), and Kuznetsov *et al.* examined NEt_4

---

[1] To whom correspondence should be sent.

0021-9517/87 $3.00

$[Fe_2Mn(CO)_{13}]$ on various supports (*39*), but no study has been made on the effect of varying the Mn/Fe ratio of supported catalysts. This is of some interest because the high selectivity to olefins has not always been achieved in these previous studies. A promising method of obtaining supported Mn/Fe catalysts is the use of organometallic mixed-metal carbonyl clusters as the metal precursor (*40–42*). The utilization of these clusters has a number of advantages such as (1) uniformly supported clusters can be obtained with stoichiometric metal ratios, namely, Mn_2, Mn_2Fe, MnFe, $MnFe_2$, and Fe_3; (2) promoters can be added to the clusters by preparing the potassium salts of the carbonyl clusters, which also ensures intimate metal contact; and (3) zero-valent metals can be initially obtained on appropriate supports by decarbonylation of the clusters at mild temperatures (475 K) (*42*), which can also enhance dispersion.

High-surface-area carbon has certain properties that make it an attractive support for Fischer–Tropsch catalysts. The high surface area within the small pores allows the distribution of the carbonyl clusters and stabilizes highly dispersed Fe particles (*16*), presumably due to the presence of physical barriers which suppress surface migration and resultant agglomeration. The carbon can be made virtually sulfur free by high-temperature reduction in H_2 which, in addition, also eliminates surface hydroxyl and carboxyl groups.

The preparation, characterization, and catalytic behavior of a family of carbon-supported Fe, Mn, Fe/Mn, and Fe/Mn/K cluster catalysts are described in this paper, with an emphasis on those catalysts which gave unusually high selectivities to light-weight olefins. The following paper discusses activity maintenance and regenerability (*55*).

EXPERIMENTAL

The high-surface-area amorphous carbon black (CSX-203, Cabot Corp., 1400 m^2/g) used as a support in this study had an initial sulfur content of 0.59 wt% which was reduced to 0.13% by treating in H_2 at 1223 K for 12 h (*17, 42*). The carbon was heated to 573 K under a dynamic vacuum of 10^{-4} kPa for 8 h prior to impregnation to remove any physisorbed water. Using published procedures, the following clusters were synthesized: $Mn_2(CO)_{10}$, $Mn_2Fe(CO)_{14}$ (*43*), $NEt_4[FeMn(CO)_9]$ (*44*), $NEt_4[Fe_2Mn(CO)_{13}]$ (*44*), $Fe_3(CO)_{12}$, $K[MnFe(CO)_9]$ (*44*), $NEt_4[Fe_2Mn(CO)_{13}]$ (*44*), and $K[HFe_3(CO)_{11}]$ (*45*). These were supported on the carbon by incipient wetness impregnation using dry and degassed THF as solvent. The $Mn_2(CO)_{10}$ + $Fe_3(CO)_{12}$ catalyst with Mn/Fe = 2 was prepared by sequential impregnation of the two clusters, using $Mn_2(CO)_{10}$ first. A coimpregnated catalyst was prepared using the same two carbonyls in a single solution with a metal ratio of Fe/Mn = 2. The impregnations were done under N_2 using standard Schlenk techniques (*46*), and the catalysts were dried by evacuating to 10^{-4} kPa for 8 h at 300 K. The chemisorption cells and microreactor were loaded in a N_2-filled glove box, thus eliminating air exposure. Metal loadings were determined using neutron activation analysis which showed close agreement with the cluster stoichiometries.

All fresh catalysts were subjected to two different pretreatments prior to adsorption or kinetic measurements—a low-temperature reduction (LTR), which consisted of heating to 473 K under flowing He (40 cc/min) for the kinetic runs or under dynamic vacuum ($<10^{-4}$ kPa) for the chemisorption measurements and reducing in H_2 at this temperature for 2–5 h until no solvent could be detected in the gas stream by gas chromatography, and a high-temperature reduction (HTR), which consisted of heating to 673K under flowing H_2 (40 cc/min) and reducing at 673 K in H_2 for 16 h. A dynamic H_2 desorption measurement was conducted, as described later, and the catalyst was then evacuated for 1 h at 473 K and cooled to 195 K (dry ice–acetone bath) under vacuum for CO chemisorption measurements. The sample was heated under vacuum to 473 K and reduced under flowing H_2 for 2 h. The cell was evacuated for 1 h at 473 K, cooled to 300 K, and a CO chemisorption at 300 K was conducted. The sample was then heated to 673 K under vacuum and reduced in H_2 for 16 h. The exact sequence of steps was then followed as for the LTR, but with the sample being reduced at 673 K for 16 h, rather than 473 K for 2 h. Chemisorption measurements on the used samples consisted of only the HTR sequence.

The H_2 desorption technique was essentially that used by Amelse *et al.* (*47*). The cell was cooled under flowing H_2 from the reduction temperature of either 473 or 673 K to 273 K, evacuated for 10 min, and then heated to the original reduction temperature in a closed, known volume. The amount of H_2 desorbed was determined from the pressure, measured after both 20- and 60-min periods. A dual-isotherm method was used for the CO chemisorption at both 195 and 300 K, with irreversible CO being determined at a pressure of 200 Torr (26.7 kPa). During CO chemisorption measurements the first data point was taken after the pressure had stabilized, which occurred between 15 and 90 min, while subsequent points equilibrated faster and could be taken after 10–30 min. Details of the adsorption system, capable of vacuums below 10^{-6} Torr, have been given elsewhere (*48*).

The kinetic data were obtained at 1 atm (100 kPa) under differential reaction conditions in a glass plug–flow reactor using a Perkin–Elmer Sigma 3 gas chromatograph fitted with Chromosorb 102 columns, as described previously (*16*, *48*). The conversion of CO to hydrocarbon (HC) products was kept below 7%, and both rates and activation energies were obtained for the most active catalyst, $Fe_3(CO)_{12}$, at different space velocities to show that mass transfer was not a problem. Catalyst charges to the reactor were 0.35 to 0.55 g. Each set of kinetic data was obtained after a 20-min exposure to the reactant gases using an H_2 bracketing technique consisting of a 20-min H_2 reduction period between subsequent points (*49*). Helium was used as a diluent gas when partial pressure studies were done. The purities of the gases used were H_2, 99.999% (M. G. Scientific), CO, 99.99%, (Matheson purity) and He, 99.999% (M. G. Scientific). For further purification the H_2 was passed through a molecular sieve and an Oxytrap (Alltech Asso.), the He through a molecular sieve, a Drierite tube, and a GE Go Getter, and the CO through a heated molecular sieve trap. All catalysts were characterized by X-ray diffraction using a Philips XRG-3000 diffractometer with Cu*K*α radiation.

RESULTS

Chemisorption

The catalysts studied and their metal loadings are listed in Table 1, and the CO and H_2 uptakes on the fresh and used samples are reported in Tables 2 and 3, respectively. The chemisorptions are normalized to the amount of Fe present in the catalyst for the fresh and used catalysts, but are also presented for the fresh catalysts on the basis of total metal content (Mn + Fe). The chemisorption measurements on the used catalysts were repeated several times and two sets of data are given in Table 3. The first set of chemisorption measurements (Run 1) was obtained shortly after the completion of the kinetic studies while the second set (Run 2) was obtained after a longer period of exposure to the air. The evacuation time between isotherms at 195 K for the first set of data of the used catalysts was 5–10 min, which proved to be insufficient to remove all the physisorbed CO as determined later by CO adsorption at 195 K on the pure support; therefore, these results are not listed. A 1-h evacuation time was found to be required to completely remove physically adsorbed CO due to pore diffusion, and this time was subsequently used for the second set of chemisorptions (Run 2). This effect was not observed at 300 K since adsorption on the pure carbon alone showed no irreversible uptake after only a 10-min evacuation. We have therefore cho-

TABLE 1

Percentage Metal Loadings of CSX-203-Supported Catalysts

Carbonyl clusters	wt% metal[a]			µmole metal/ g catalyst			Ratio (Mn/Fe)
	Mn	Fe	Total	Mn	Fe	Total	
$Mn_2(CO)_{10}$	2.56	—	2.56	466	0	466	High
$Mn_2Fe(CO)_{14}$	1.35	0.64	1.98	245	114	359	2.15
$NEt_4[MnFe(CO)_9]$	1.54	1.53	3.08	281	275	556	1.02
$NEt_4[MnFe_2(CO)_{13}]$	1.64	3.13	4.78	299	561	860	0.53
$Fe_3(CO)_{12}$	—	3.78	3.78	0	678	678	0
$K[MnFe(CO)_9]$	1.33	1.16	2.50	236	203	439	1.16
$K[MnFe_2(CO)_{13}]$	0.98	2.03	3.01	178	364	542	0.49
$K[HFe_3(CO)_{11}]$	—	4.38	4.38	—	786	786	0
2Mn/Fe; carbonyls	3.06	1.52	4.59	557	273	830	2.04
2Fe/Mn; nitrates	1.37	2.09	3.46	250	377	627	0.66
2Fe/Mn; carbonyls[b]	1.25	2.50	3.75	228	448	676	0.50

[a] Analyses were done on both the fresh and used catalysts. The reported values are weighted averages.

[b] Metal loading was estimated from the amount of $Fe_3(CO)_{12}$ and $Mn_2(CO)_{10}$ impregnated.

sen the first set (Run 1) of CO chemisorption at 300 K as being the best values for the calculation of dispersions for the catalysts, and we will define our Fe dispersion as the CO (300 K)/Fe_{total} ratio. In the second set of values (Run 2), the evacuation time at 195 K was 1 h; consequently, this set of data is better to obtain the CO (300 K)/CO (195 K) ratio for the used catalysts. From the CO chemisorption values it is clear that no CO adsorbs on the Mn catalyst at 300 K.

An important pattern in the data (Table 2) is the drastic increase in chemisorption values when using an HTR step rather than

TABLE 2

Chemisorption Measurements on Fresh Catalysts

Carbonyl clusters	µmole/µmole (Fe + Mn)				µmole/µmole Fe			
	LTR		HTR		LTR		HTR	
	H_2[a]	CO 300 K	H_2[b]	CO 300 K	H_2[a]	CO 300 K	H_2[b]	CO 300 K
$Mn_2(CO)_{10}$	0.07	0.002	0.06	0.002	—	—	—	—
$Mn_2Fe(CO)_{14}$	0.008	0.006	0.04	0.28	0.03	0.02	0.13	0.90
$NEt_4[MnFe(CO)_9]$	0.02	0.02	0.06	0.30	0.04	0.04	0.11	0.60
$NEt_4[MnFe_2(CO)_{13}]$	0.05	0.02	0.08	0.27	0.08	0.02	0.13	0.42
$Fe_3(CO)_{12}$	0.07	0.53	0.09	0.90	0.07	0.53	0.09	0.90
$K[MnFe(CO)[_9]$	0.04	0.02	0.14	0.10	0.09	0.04	0.30	0.22
$K[MnFe_2(CO)_{13}]$	0.05	0.05	0.13	0.27	0.08	0.08	0.20	0.40
$K[HFe_3(CO)_{11}]$	0.04	0.30	0.06	0.41	0.04	0.30	0.06	0.41
2Mn/Fe; carbonyls	0.03	0.02	0.05	0.09	0.10	0.06	0.18	0.26
2Fe/Mn; nitrates	—	—	0.12	0.69	—	—	0.20	1.15
2Fe/Mn; carbonyls	0.06	—	0.07	0.35	0.09	0.50	0.10	0.53

[a] Via desorption to 473 K (see text).

[b] Via desorption to 673 K (see text).

TABLE 3

Chemisorption Measurements after HTR on Used Catalysts (after Kinetic Studies)

Carbonyl clusters	μmole/μmole Fe					CO (300 K)/ CO (195 K)
	Run 1		Run 2[a]			
	H_2	CO 300 K	H_2	CO[b] 195 K	CO 300 K	
$Mn_2(CO)_{10}$[c]	0.02	0.00	0.07	0.03	0.00	0.0
$Mn_2Fe(CO)_{14}$	0.09	0.62	0.14	0.14	0.32	2.3
$NEt_4[MnFe(CO)_9]$	0.13	0.51	0.14	0.13	0.26	2.0
$NEt_4[MnFe_2(CO)_{13}]$	0.09	0.33	0.08	0.08	0.16	2.0
$Fe_3(CO)_{12}$	0.10	0.54	0.08	0.07	0.10	1.5
$K[MnFe(CO)_9]$	0.30	0.14	0.17	0.19	0.15	0.8
$K[MnFe_2(CO)_{13}]$	0.14	0.14	0.12	0.15	0.12	0.8
$K[HFe_3(CO)_{11}]$	0.05	0.04	—	—	—	—
2Mn/Fe; carbonyls	0.09	0.40	0.09	0.15	0.31	2.1
2Fe/Mn; nitrates	—	—	0.11	0.15	0.97	6.4
2Fe/M; carbonyls	—	—	0.09	0.20	0.35	1.8

[a] See chemisorption results section.

[b] Evacuated 60 min between isotherms.

[c] Based on Mn content; μmole/μmole Mn.

an LTR treatment. The CO (300 K) values increase by factors of 5 to 50 except for the catalysts containing no Mn—$Fe_3(CO)_{12}$ and $K[HFe_3(CO)_{11}]$, which showed increases by factors of only 1.7 and 1.4, respectively. When these chemisorption values are normalized to the amount of iron present, the variation among the apparent dispersions of the fresh samples after HTR is between 0.42 and 0.90 for the catalysts without K, and all samples after HTR are very well dispersed. After an LTR step, however, the variation in CO (300 K)/Fe_{total} is between 0.02 and 0.53, with all the catalysts except $Fe_3(CO)_{12}$ and $K[HFe_3(CO)_{11}]$ having values less than 0.08, and the values are now approximately an order of magnitude lower than that obtained for the $Fe_3(CO)_{12}$ catalyst. This indicates a chemisorption suppression after the LTR step due either to incomplete decarbonylation of the mixed clusters or to a Mn–Fe interaction which is overcome to a large extent after the HTR treatment. The latter possibility implies metal segregation during the HTR treatment, in agreement with the work of Jensen and Massoth who suggested formation of a two-phase system with Mn oxide platelets covering iron particles (*32, 33*), where the Fe-phase was formed by agglomeration initiated at high temperature (*34*).

The first set of CO (300 K) values for the used unpromoted catalysts compare favorably with the CO (300 K) values for the fresh samples, suggesting that little sintering occurred under reaction conditions. For example, only a small drop in dispersion from 0.60 to 0.51 was indicated for the NEt_4 $[FeMn(CO)_9$ catalyst after 120 h on-stream at 587 K; however, iron crystallite sizes were not calculated due to the presence of the Mn in these catalysts. The Mn is expected to be oxidized and in contact with the Fe so that the choice of an atomic diameter needed for the calculation is unclear. In addition, recent investigations by Phillips *et al.* (*50, 51*) and by Kaminsky *et al.* (*42*) have indicated that carbon-supported iron catalysts prepared from carbonyl clusters may be present in raft-like structures, rather than spheroids. Regardless, the dispersion values between 0.22 and 0.90 indicate that efficient use of the Fe is obtained and very small Fe-containing particles exist in this family of catalysts. This conclusion is supported by the fact that no X-ray diffraction peaks were obtained for the catalysts either before or after reaction.

The CO (300 K)/CO (195 K) ratio for the used catalysts after a 1-h evacuation at 195 K was consistently near 2 for the unpromoted catalysts, which is close to previous ratios for Fe-only catalysts (*42, 48*). However, this ratio was noticeably lower for the two K-promoted Fe–Mn catalysts. The high value of 6.4 for the 2Fe/Mn catalyst prepared from nitrates is attributed to subcarbonyl formation (*42*). It is important to note that the CO chemisorption values decreased from Run 1 to Run 2 for all of the catalysts whereas the H_2 uptakes remained relatively stable. Since little sintering occurred during reaction conditions and reduction at 673 K, little sintering is expected during successive chemisorption measurements, as indicated by the H_2 uptakes. We believe that this decrease in CO uptake may be a consequence of Fe carbide formation during the heating step *in vacuo* to 673 K after the CO chemisorption experiment as CO is known to dissociate on Fe at temperatures above 300 K (*52*). This would decrease CO chemisorption but have a much smaller effect on H_2 chemisorption as discussed later. These difficulties illustrate the importance of pretreatment procedures used for adsorption or kinetic studies.

Hydrogen adsorption on all the fresh and used catalysts after HTR gave H/Fe_{total} ratios within a factor of 5 of those obtained from CO adsorption at 300 K, and for 12 out of 18 cases this ratio was less than 3. Although the agreement is not very close, it is a substantial improvement over static hydrogen adsorption measurements which have been previously employed (*17, 42*).

Kinetic Studies

Specific activities and turnover frequencies (TOFs) of the catalysts are reported in Table 4 for both the LTR and HTR pretreatments. The $Mn_2(CO)_{10}$ sample had no activity after either treatment, thus confirming that Mn oxides are inactive CO hydrogenation catalysts (*29–31*). The turnover frequencies in Table 4 are based on CO chemisorption at 300 K on the fresh catalysts after either pretreatment and therefore present minimum values. The TOFs were higher after LTR than after HTR for all Mn-containing catalysts although activities (per g Fe) were lower after the LTR step. This is a consequence of the lower chemisorption obtained after an LTR pretreatment; however, it clearly demonstrates that active catalysts can be obtained without the use of an HTR step typically required for iron. The activity of the sequentially impregnated $Fe_3(CO)_{12}/Mn_2(CO)_{10}$ (2Mn/Fe) sample was substantially higher than that of the $Mn_2Fe(CO)_{14}$ carbonyl cluster and nearer that of the Fe-only sample, indicating that a greater extent of interaction between the Fe and Mn is achieved using stoichiometric clusters.

From Table 4 it is clear that the addition of Mn to Fe clusters (without K) diminished the activity, even when normalized to the iron present, the latter of which is contrary to the trend observed by Schulz and coworkers for bulk catalysts (*29–31*). The addition of K to the MnFe and $MnFe_2$ clusters enhanced specific activity and had little effect on TOF values, contrary to the behavior found with more active Fe–Co clusters (*53*), but consistent with older work on multiply-promoted iron Fischer–Tropsch catalysts (*3, 54*). The addition of a K atom to the $Fe_3(CO)_{12}$ cluster produced a small decrease in specific activity, almost no change in TOF, and an increase in CO_2 production, similar to the K promotion of the MnFe and $MnFe_2$ clusters.

A typical set of selectivity results at low CO conversion is reported in Table 5 after both low- and high-temperature reductions. It is clear that the average molecular weight of the products decreases as the Mn content increases, indicating that the chain-growth probability, α, decreases; however,

TABLE 4

Catalytic Activities of Carbon-Supported Clusters for CO Hydrogenation after LTR and HTR: $T = 548$ K, $P = 100$ kPa, $H_2/CO = 3$

Initial cluster	CO conversion[a] (%)	Activity[a] (μmol CO/ g cat · s)	Activity ((μmole CO reacted/ μmole Fe · s) × 10^3)				TOF[b] ($s^{-1} \times 10^3$)	
			Total	CO_2	HC	CH_4	HC	CH_4
LTR								
$Mn_2(CO)_{10}$	0	0	0.004	0.004	—	—	0	0
$Mn_2Fe(CO)_{14}$	0.06	0.005	0.077	0.036	0.042	0.042	2.4	0.2
$NEt_4[MnFe(CO)_9]$	0.05	0.004	0.033	0.033	0.013	0.003	0.3	0.1
$NEt_4[MnFe_2(CO)_{13}]$	1.30	0.14	0.51	0.27	0.24	0.059	10.8	2.7
$Fe_3(CO)_{12}$	2.7	0.58	1.61	0.76	0.86	0.16	1.6	0.3
$K[MnFe(CO)_9]$	1.3	0.04	0.70	0.52	0.18	0.06	4.7	1.6
$K[MnFe_2(CO)_{13}]$	0.8	0.08	1.79	1.29	0.50	0.07	6.5	1.0
$K[HFe_3(CO)_{11}]$	2.2	0.34	1.55	1.11	0.44	0.05	1.6	0.2
2Mn/Fe; carbonyls	0.8	0.04	0.32	0.18	0.15	0.05	2.7	0.9
2Fe/Mn; nitrates	—	—	—	—	—	—	—	—
2Fe/Mn; carbonyls	0.8	0.10	0.40	0.18	0.22	0.10	1.5[c]	0.7[c]
HTR								
$Mn_2(CO)_{10}$	0	0	0.006	0.006	—	—	0	0
$Mn_2Fe(CO)_{14}$	0.5	0.007	0.12	0.06	0.06	0.02	0.07	0.02
$NEt_4[MnFe(CO)_9]$	0.4	0.05	0.55	0.38	0.17	0.03	0.3	0.05
$NEt_4[MnFe_2(CO)_{13}]$	2.4	0.52	1.66	0.75	0.91	0.20	2.2	0.5
$Fe_3(CO)_{12}$	2.0	0.80	2.24	1.06	1.17	0.23	1.3	0.3
$K[MnFe(CO)_9]$	1.4	0.08	1.46	1.06	0.41	0.04	1.9	0.2
$K[MnFe_2(CO)_{13}]$	1.7	0.29	2.46	1.68	0.78	0.10	2.0	0.2
$K[HFe_3(CO)_{11}]$	6.1	0.60	1.90	1.15	0.77	0.12	1.9	0.3
2Mn/Fe; carbonyls	1.8	0.90	0.69	0.36	0.34	0.09	1.3	0.3
2Fe/Mn; nitrates	1.9	0.20	1.08	0.56	0.52	0.13	0.5	0.1
2Fe/Mn; carbonyls	4.1	0.22	0.98	0.49	0.50	0.10	0.9	0.2

[a] CO converted to hydrocarbons (HC) only.

[b] Based on CO adsorption at 300 K on fresh samples (molecule CO reacted).

[c] Based on CO (195 K); $CO/Fe_s = 1:2$.

precise α values could not be calculated because only trace amounts of medium molecular weight products were formed. Heavier products are favored after HTR over all the Mn-containing catalysts, indicating that the Fe–Mn catalysts become more iron-like after an HTR step. The olefin-to-paraffin ratio (OPR) for the C_2 and C_3 products after the LTR shows that very high selectivities can be obtained, even for certain unpromoted catalysts such as that prepared from $NEt_4[Fe_2Mn(CO)_{13}]$ and the coimpregnated 2Fe/Mn carbonyl catalyst. High OPRs have also been reported by Bruce, Hope, and Turney (*38*) and Kuznetsov *et al.* (*39*) for the $NEt_4[Fe_2Mn(CO)_{13}]$ cluster on oxide supports. It is important to note that this selectivity is very dependent upon the pretreatment used. For these two catalysts with an Fe/Mn ratio of 2, the OPRs drop from 6.4 and 3.9 after LTR to initial values of 1.0 and 0.7 after HTR, respectively. These latter values are in reasonable agreement with that for $Fe_3(CO)_{12}$ on carbon and indicate that a surface phase separation to metallic iron and MnO may have occurred during HTR. The nitrate-derived catalyst with Fe/Mn = 2 did not show an enhanced OPR, which again demonstrates the importance of using the metal

TABLE 5

Selectivity of CO Hydrogenation after LTR and HTR Pretreatments of Carbon-Supported Fe–Mn and K–Fe–Mn Catalysts: P = 100 kPa, H_2/CO = 3

Initial Cluster	Temperature (°C)	CO conversion to HC (%)	Selectivity (HC mole%)								OPR $\left(\frac{\Sigma C_{2,3}^{2-}}{\Sigma C_{2,3}}\right)$	$(CO - CO_2)/(CO - HC)$
			C_1	C_2^{2-}	C_2	C_3^{2-}	C_3	C_4^{2-}	C_4	C_5^+		
LTR												
$Mn_2(CO)_{10}$	327	0	—[a]	—	—	—	—	—	—	—	—	High
$Mn_2Fe(CO)_{14}$	300	0.06	100	—	—	—	—	—	—	—	—	0.7
$NEt_4[MnFe(CO)_9]$	306	0.21	37	29	24	10	—	—	—	—	1.6	1.8
$NEt_4[MnFe_2(CO)_{13}]$	275	1.3	43	26	7	19	—	5	—	—	6.4	0.9
$Fe_3(CO)_{12}$	249	2.7	40	11	12	15	8	—	5	9	1.3	0.7
$K[MnFe(CO)_9]$	302	1.3	38	31	—	13		12	—	6	High	2.6
$K[MnFe_2(CO)_{13}]$	250	0.8	31	33	—	23	—	14	—	—	High	2.9
$K[HFe_3(CO)_{11}]$	280	2.2	37	28	—	20	—	9	—	6	High	2.3
2Mn/Fe; carbonyls	300	0.8	50	22	11	17	—	—	—	—	3.5	1.4
2Fe/Mn; nitrates	—	—	—	—	—	—	—	—	—	—	—	—
2Fe/Mn; carbonyls	284	1.0	61	18	8	13	—	—	—	—	3.9	0.9
HTR												
$Mn_2(CO)_{10}$	348	0	—	—	—	—	—	—	—	—	—	High
$Mn_2Fe(CO)_{14}$	314	0.52	50	17	19	9	6	—	—	—	1.0	0.9
$NEt_4[MnFe(CO)_9]$	309	1.3	38	22	15	17	9	—	—	—	1.6	1.8
$NEt_4[MnFe_2(CO)_{13}]$	251	2.4	48	10	16	12	6	—	7	1	1.0	0.8
$Fe_3(CO)_{12}$	225	2.0	42	11	12	14	6	2	5	8	1.4	0.5
$K[MnFe(CO)_9]$	290	1.4	25	35	—	30	—	11	—	—	High	2.4
$K[MnFe_2(CO)_{13}]$	250	1.7	28	29	—	24	—	11	—	8	High	2.4
$K[HFe_3(CO)_{11}]$	285	1.9	41	27	3	20	—	8	—	3	15.7	1.7
2Mn/Fe; carbonyls	300	1.8	47	15	16	10	5	—	4	3	1.2	1.2
2Fe/Mn; nitrates	279	2.2	43	10	18	10	7	—	7	4	0.8	1.0
2Fe/Mn; carbonyls	260	2.2	46	9	19	9	7	—	6	5	0.7	1.0

[a] — indicates that no such product was detected.

carbonyl clusters as catalyst precursors. The sequentially impregnated sample also showed a marked drop in selectivity after HTR, indicating a reduction in Mn–Fe interaction after this pretreatment.

After HTR, the OPRs of 1.6 and 1.0 for C-supported $NEt_4[FeMn(CO)_9]$ and $NEt_4[Fe_2Mn(CO)_{13}]$, respectively, were obtained after 20 min on-stream at the temperatures shown, but these ratios increased to 3 or more during activity maintenance runs (*55*). The addition of K to these two clusters increased the olefin selectivity to such an extent that no paraffins, other than CH_4, could be detected, and this result was independent of pretreatment. For the best catalysts, such as KMnFe/C after an HTR step, the hydrocarbon product distribution on a wt% (carbon utilization) basis was 11% methane, 31% ethylene, 39% propylene, and 20% butene. Addition of K to the $Fe_3(CO)_{12}$ cluster also increased the selectivity of olefins such that only 37 mole% of the product consisted of CH_4 after LTR. This high selectivity to light olefins dropped somewhat after HTR as 3 mole% ethane and 3% C_{5+} products were detected. For all of the K-containing catalysts and many of the Fe–Mn catalysts, such as $NEt_4[Fe_2Mn(CO)_{13}]$/C, the OPR remained high for long periods on-stream, as discussed in the second paper in this series (*55*).

The presence of carbon deposition during the CO hydrogenation reaction is indicated by the last column in Table 5. Assuming that H_2O is a primary product and it is completely converted to CO_2 via the water gas shift reaction, the maximum ratio of the moles CO_2 formed to the moles CO reacted to hydrocarbons, $(CO - CO_2)/(CO - HC)$, is 1 in the absence of carbon deposition and other reactions to produce CO_2. Therefore, a $(CO - CO_2)/(CO - HC)$ ratio greater than unity indicates carbon deposition via CO disproportionation but a ratio less than 1 does not preclude this reaction. It is clear that the incorporation of K into the clusters facilitates carbon deposition, which may be attributed to an increased heat of chemisorption for CO (*56–58*). This behavior is the most negative aspect of K promotion, but does decrease somewhat after the HTR is used, and it also decreases to give ratios below 2 after several hours on-stream (*55*). Utilization of increased pressures may provide a way to circumvent this problem, as Schulz and Gökcebay showed that the (CO − CO_2)/(CO − HC) ratio decreased from 0.7 to 0.05 when the pressure was increased from 3 to 90 bar, while the fraction of olefins only dropped from 0.82 to 0.64 for a bulk Fe–Mn catalyst (*29*).

The activation energies and partial pressure dependencies are listed in Table 6. The activation energies were obtained by taking the arithmetic average of those obtained during runs of both increasing and decreasing temperature to average out any deactivation. The pretreatment does not affect activation energies markedly, with the exception of the Mn_2Fe/C and MnFe/C catalysts, and after the HTR step all but one falls between 80 and 105 kJ/mole, which are typical values for iron (*17, 59*). The wider variation after a LTR step may indicate a less iron-like state of the catalyst.

The partial pressure analyses were done at different temperatures (533–583 K) so that reasonable conversions (0.1–10%) could be obtained. To compare pressure de-

TABLE 6

Activation Energies and Partial Pressure Dependencies of C-Supported Catalysts

Initial cluster	Activation energies (kJ/mole)			Pressure dependence for methanation[a]	
	CO − HC	CO − CH_4	CO − CO_2	x	y
LTR					
$Mn_2(CO)_{10}$	—	—	75		
$Mn_2Fe(CO)_{14}$	138	138	26		
$NEt_4[MnFe(CO)_9]$	145	121	85		
$NEt_4[MnFe_2(CO)_{13}]$	86	69	82		
$Fe_3(CO)_{12}$	71	63	86		
$K[MnFe(CO)_9]$	124	99	92		
$K[MnFe_2(CO)_{13}]$	94	95	98		
$K[HFe_3(CO)_{11}]$	—	—	—		
2Mn/Fe; Carbonyls	93	79	99		
2Fe/Mn; Nitrates	—	—	—		
2Fe/Mn; Carbonyls	80	77	95		
HTR					
$Mn_2(CO)_{10}$	—	—	42	—	—
$Mn_2Fe(CO)_{14}$	90	86	90	1.6	−0.6
$NEt_4[MnFe(CO)_9]$	105	109	91	1.1	−0.2
$NEt_4[MnFe_2(CO)_{13}]$	91	81	101	1.3	−0.2
$Fe_3(CO)_{12}$	82	73	90	1.3	−0.2
$K[MnFe(CO)_9]$	136	111	98	1.5	−1.0
$K[MnFe_2(CO)_{13}]$	90	88	84	1.6	−0.5
$K[HFe_3(CO)_{11}]$	89	83	97	1.3	−0.4
2Mn/Fe; Carbonyls	87	82	96	1.6	−0.3
2Fe/Mn; Nitrates	104	80	93	1.3	−0.1
2Fe/Mn; Carbonyls	80	75	88	1.4	−0.2

[a] x and y ($r = kP_{H_2}^{x}P_{CO}^{y}$) were corrected to obtain values at a constant temperature of 548 K.

pendencies at a single temperature (548 K), the temperature dependencies of x and y ($r = kP_{H_2}^{x}P_{CO}^{y}$) were determined for $Fe_3(CO)_{12}$, and parallel curves were assumed for the other catalysts. The range of dependencies listed in Table 6, 1.1–1.6 for H_2 and −0.2 to −1.0 for CO, encompass the range of previously reported values for methanation and hydrocarbon formation (*17, 42, 59*). The most iron-like catalysts had dependencies near 1.2 for H_2 and −0.2 for CO, in excellent agreement with previous work (*17*), while the catalysts with K and/or a Mn/Fe ratio near 2 had more positive H_2 and more negative CO dependencies. However, the dependence on total pressure was consistently near first order for all catalysts.

DISCUSSION

Chemisorption

Hydrogen adsorption is known to be activated on bulk promoted iron catalysts (*60*), and the activation barrier has recently been found to be even more pronounced on small supported iron crystallites (*48, 61, 62*). Static hydrogen chemisorption techniques thus do not yield significant uptakes near 300 K (*48, 63*); however, the dynamic desorption technique introduced by Amelse *et al.* (*47*) minimizes this problem and provides a method to count surface Fe atoms (Fe_s) (*64*).

No standard technique exists for CO chemisorption on iron, but good agreement has been obtained among different techniques for crystallite size estimates by assuming bridge-bonded CO at 195 K, i.e., CO (195 K)/Fe_s = 0.5 (*48, 65*). Because the strongly adsorbed CO at 195 K is obtained by the subtraction of two large numbers due to the high degree of physisorption, the intrinsic error is relatively large compared to that at 300 K, where physisorption on the carbon is much lower. Consequently CO chemisorption at 300 K may be a more precise measure of Fe surface area in this study. As the CO (300 K)/CO (195 K) ratio has been reported to have a value near 2, a CO (300 K)/Fe_s adsorption ratio near 1.0 at 300 K appears reasonable (*42, 48*). Subcarbonyl formation has been reported for highly dispersed Group VIII metals (*48, 66–69*), and although its presence cannot be complete discounted, the presence of Mn or Mn oxide on the Fe surface could readily inhibit its formation. CO chemisorption on Fe_3O_4 and Fe carbides is relatively weak and can be pumped off during evacuation at 300 K (*70*), and Boudart *et al.* found that MgO-supported Fe_2O_3 did not strongly chemisorb CO since it could be pumped off at 300 K (*65*). Consequently, significant irreversible CO adsorption at 300 K is expected only on reduced iron.

Only two chemisorption studies related to Mn or Mn oxides had been reported before 1970 (*71*)—Taylor and Williamson found that H_2 adsorption was activated and very low on Mn oxides (*72*), and Trapnell and co-workers also reported limited, weak H_2 chemisorption (*73*). More recently Bickley *et al.* found that H_2 chemisorbs dissociatively on metallic Mn at 78 K and desorbs at 295 K (*74*). Studies by Lohrengel and Baerns (*20*), Barrault *et al.* (*35, 37*), and Jensen and Massoth (*32*) have consistently shown that incorporation of Mn into iron catalysts markedly suppresses CO chemisorption. The chemisorption results reported here are apparently the first for supported, well-dispersed Fe/Mn particles.

The CO chemisorption at 300 K on the fresh catalysts reported here increased drastically (5- to 50-fold) after the HTR procedure, which we interpret to mean that intimate contact existed initially between Mn and Fe after the LTR step, resulting in suppressed chemisorption, which is consistent with previous work (*20, 32, 35, 37*). The HTR led to a segregation of metallic iron from the Mn oxide phase which increased the free Fe surface area and hence the chemisorption. The CO (300 K)/CO (195 K) ratios near 2 for the used unpromoted catalysts after the HTR step are also consistent with the behavior of small Fe crystallites on carbon (*17, 48*). The decrease in CO uptake during successive measurements is not attributed to sintering, but to Fe carbide formation during the heating step *in vacuo* to 673 K following the CO chemisorption measurements as CO dissociation occurs readily on Fe surfaces at temperatures above 300 K (*52*). Residual iron oxides will not be carburized because of the lack of solubility of carbon (*75*). Although the removal of iron carbide is thermodynamically possible at 673 K in H_2 (*76*), it may be kinetically limited. Raupp and Delgass showed that the initial carburization of Fe/SiO_2 and Fe/MgO was a fast process for small particles (<10 and <4 nm, respectively), but the subsequent hydrogenation at 573 K in H_2 was a slow process and only 30% of the Fe carbide was reduced to metallic Fe in 10 h (*77*). Carbide remaining after the HTR following the heating step *in vacuo* could decrease the CO chemisorption at both 195 and 300 K, but would have a relatively small effect on the H_2 adsorption (*70*).

Catalytic Behavior

Iron and cobalt are active FT catalysts but possess limited selectivity. While the adjustment of reaction parameters can help maximize the production of medium-chain olefins, the capability to attain high selectivity to C_2 to C_4 olefins depends on the development of new catalysts (*3*). Their hydrogenation activity must not be too high as this would increase CH_4 formation and hydrogenate primary olefinic products to paraffins. These catalysts may also have to be operated in higher temperature regimes than conventional catalysts where olefins are thermodynamically favored over paraffins. The Mn–Fe catalysts described here were investigated with these considerations in mind.

The most significant result of this study is the preparation of highly dispersed Fe–Mn catalysts which have selectivities to C_2–C_4 olefins as high as 85–90 wt%, with the balance being CH_4. No other paraffins were detected. For example, KFe_2Mn/C after LTR and KFeMn/C after HTR gave 11–14 wt% methane, 30–31 wt% ethylene, 31–39 wt% propylene, and 20–25 wt% butene. These high olefin yields remained constant during long periods (20–40 h) on-stream (*55*). Although certain FeMn/C catalysts were quite active and had high OPRs after an LTR pretreatment, in particular the Fe_2Mn catalyst, the activity and selectivity of these olefin-producing catalysts were increased by using potassium as a counter ion in the carbonyl clusters, but these enhancements by K carry with them the price of increased CO_2 production. However, improvements may be obtained by operation at higher pressures. The optimum choice between the less active and selective unpromoted catalyst and the K-promoted catalyst has yet to be determined.

The catalytic behavior of the Fe–Mn catalysts described here can be compared to that reported by others, namely, Barrault *et al.* (*35–37*), Bruce, Hope, and Turney (*38*), Deckwer and co-workers (*23, 24*), van Dijk *et al.* (*12*), Satterfield *et al.* (*27, 28*), Schulz *et al.* (*29–31*), and Kuznetsov *et al.* (*39*). The reaction conditions are summarized in Table 7 while the activity and selectivity comparisons are made in Fig. 1. The activity and selectivity of the *best* catalysts were taken from each study, even though they sometimes represented different catalysts after different treatments in the same study. The best choice of a basis for comparing activity is not obvious, but we have chosen specific activity (moles of CO-to-HC products per mole of iron per second) because turnover frequencies have not been reported in the other studies and, in addition, Fe loadings vary widely. On this basis it is clear that the selectivities of our Fe–Mn/C catalysts are comparable to or better than any reported by other groups, even though our H_2/CO ratio is much higher, and the activities are noticeably higher. The high dispersions of these C-supported catalysts promote high specific activities, of course, but turnover frequencies on small iron crystallites are markedly lower than on large crystallites (*17, 48*). The catalyst with the most competitive activity was that of Schulz, but it was mea-

TABLE 7

Reaction Conditions during Previous Studies of FeMn Catalysts

Study[a]	Mn/Fe	P (atm)	T (°C)	H_2/CO
This study	0–2	1	275	3
1. Barrault *et al.* (*35–37*): Fe°–Fe^{3+}/MnO, MnO_2	High	1	280	1
2. Bruce *et al.* (*38*): $MnFe_2/SiO_2$	0.5	2–5	300	1.5
3. Deckwer *et al.* (*23, 24*): Bulk (Coppt)	11	2	290	0.6
4. Van Dijk *et al.* (*12*): Bulk (Coppt)	1.5	1	240	1
5. Satterfield *et al.* (*27, 28*): Bulk (Coppt)	7.3	11	280	0.8
6. Schulz *et al.* (*29–31*): Bulk (Coppt)	2–23	10	250	1.9
7. Kuznetsov *et al.* (*39*): $MnFe_2$/Various	0.5	1	250	2

[a] Coppt, Coprecipitated.

sured at 10 atm (*29*). Considering that the olefinic contents of the products from these Fe–Mn/C and K–Fe–Mn/C catalysts were comparable to those reported by previous workers but that the activity was substantially higher, these catalysts should be considered as viable alternatives for the production of low molecular weight olefins. Also, the olefin fraction in these previous studies contained large amounts of heavier hydrocarbons (C_{10+}, for example) because of the larger degree of chain growth. Finally, the stability of our catalysts under continuous reaction conditions is an additional benefit (*55*).

The evolutionary changes in these catalysts during time on-stream, the effect of LTR and HTR pretreatment, and the role of Mn is not precisely known, but some plausible speculation can be made based on previous investigations. During impregnation, the carbonyl clusters are distributed within the very small pores of the carbon (50% of the pore volume lies in pores smaller than 5 nm). Any strong interaction between the carbonyl clusters and the support is anticipated to occur at surface irregularities like steps, because very few residual surface hydroxyl and carboxyl groups will remain on the surface after the high-temperature treatment in H_2 (*78*).

During the LTR treatment in H_2 the clusters are expected to decarbonylate and to aggregate to a limited extent, such that particle sizes are similar to the diameters of the pores in which they reside. Consequently, the measured activities are not associated with the original carbonyl clusters, but with the small mixed-phase particles which form from them. Since the Fe–Mn atoms in the clusters are initially in intimate contact, this contact is presumed to remain during the LTR step. The mobility of the metal particles on the carbon surface is strongly dependent on the temperature, but since the Tammann temperatures of both components are substantially higher than 473 K, no major phase segregation is expected to

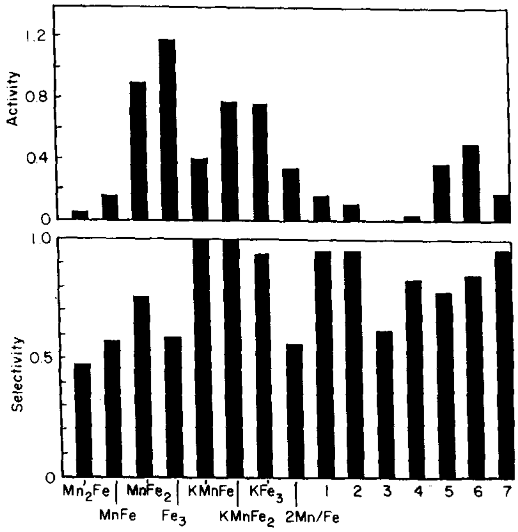

FIG. 1. Comparison of specific activity (moles of CO reacted to hydrocarbons per mole Fe per second × 10^3) and selectivity to olefins (fraction of olefins in $C_2 + C_3$ hydrocarbons) of Fe–Mn catalysts with previous results. The numbers 1–7 represent the studies and reaction conditions given in Table 7.

take place (*79*). Although both the Fe and Mn were in zero oxidation states when impregnated under O_2-free conditions, thermodynamic calculations show that Mn, in particular, requires only extremely low pressures of H_2O or O_2 for bulk oxidation; therefore, at 473 K any residual H_2O (or O_2) in the H_2 is probably sufficient to oxidize Mn to MnO or the Fe and Mn to a mixed-metal surface oxide such as Fe_2MnO_4, as discussed elsewhere (*55, 83*).

The recent studies of Baerns and co-workers have shown that the high olefin selectivity of bulk FeMn catalysts correlates with the presence of Fe_2MnO_4, which was detected by X-ray diffraction and by Mössbauer spectroscopy (*19, 21, 84*). Based on this work, we propose that the states of the catalysts before reaction in the presence of trace amounts of H_2O or O_2 are as follows: (a) if "excess" Mn is present (Mn/Fe > 0.5) a separate MnO phase can exist along with a very small amount of the transition phase $(Mn_{1-y}Fe_y)_3O_4$ ($y \ll 1$), and the Fe can be present in two phases, namely, metallic Fe and $(Fe_{1-x}Mn_x)_3O_4$ ($x \ll 1$), with the latter oxide covering a fraction of the surface; (b) when excess Fe is present (Fe/Mn > 2), the principal phases are expected to be metallic Fe and a mixed spinel, $(Fe_{1-x}Mn_x)_3O_4$ ($x < 1$), with the stoichiometry of the latter being very possibly near Fe_2MnO_4. An initial Fe/Mn ratio equal to 2 will favor formation of Fe_2MnO_4. If these phases are not completely formed prior to the introduction of the H_2/CO feed stream, we expect them to form rapidly under reaction conditions, with the activity provided only by metallic iron and/or the mixed spinel.

Metallic Fe can form both surface and bulk carbides (*77, 80–82*), and these phases have recently been observed in coprecipitated FeMn systems (*32, 33*); however, the spinel does not form carbides (*19, 20*). Consequently, at low temperatures the mixed spinel phase is stable, as suggested by thermodynamic calculations (*55, 83*). During the CO hydrogenation reaction, carbon can build up on the Fe surface in various forms such as CH_x species and other intermediates, carbidic (free) carbon, and graphitic carbon (*85–89*). All the carbon species except the graphitic phase are expected to be quite reactive with H_2, and the ease of regenerability of these Fe–Mn/C catalysts indicates not only a minimum presence of graphitic carbon, but also the absence of sintering (*55*).

The HTR step induced significantly different behavior, consistent with the work of Baerns and co-workers (*19, 20*), which implies that the mixed spinel can be reduced first to an $(Fe_{1-z}Mn_z)O$ ($z < 1$) phase and finally to metallic Fe and MnO, as expected from thermodynamics. The latter two phases have been identified by Jensen and Massoth in a coprecipitated Fe–Mn catalyst (*32*). Schulz *et al.* observed that initially alloyed Fe–Mn catalysts showed surface enrichment of MnO to a greater extent than a coprecipitated Mn–Fe catalyst (*31*); and similar results were obtained by Stencel and co-workers (*34*). This led the latter group to the conclusion that the Fe–Mn particle size might control the rate of surface Fe depletion and the extent of MnO migration (*34*). However, on the small particles in these C-supported catalysts most of the Fe surface area is available, as shown by the chemisorption measurements, so that surface segregation, rather than surface Fe depletion, is indicated. The catalyst existing after the HTR is thus expected to give a selectivity much more similar to that of iron. Recombination of MnO and Fe to form the mixed spinel is possible under reaction conditions and would increase olefin selectivity, but the amount of Fe_2MnO_4 would be expected to be less than that existing after the LTR step due to the marked initial phase separation. The chemisorption results are consistent with this hypothesis. The specific activities (per mole Fe) increased after the HTR treatment, as expected from the proposed phase changes, because metallic Fe is more active than the interacting Fe–Mn system present after the LTR step. However, the turnover frequencies decrease after the HTR due to the much higher extent of chemisorption and the premise that all surface sites are detected by CO chemisorption.

An explanation for the behavior of the $NEt_4[Fe_2Mn(CO)_{13}]$ catalyst can be offered. First, the two carbonyl-derived unpromoted catalysts with Fe/Mn = 2, together with the K-promoted clusters, were the five most selective catalysts for olefins. It seems more than coincidence that for three of them the metal ratio is that required to form the Fe_2MnO_4 mixed-metal spinel. This spinel dominates in the unpromoted catalysts after a LTR step, thereby leading to a selective olefin catalyst with moderate activity, based on the studies of Baerns and co-workers (*19*, *20*, *84*). When reduced at the higher temperature the decomposition of the spinel phase to MnO and metallic Fe provides a more active catalyst, but one with lower selectivity to light olefins. The olefin/paraffin ratio decreased from 6.4 to 1.0 and 3.9 to 0.7 while the activity increased from 0.24 to 0.91 and 0.22 to 0.50 for the $NEt_4[Fe_2Mn(CO)_{13}]$ and the 2Fe/Mn carbonyl-derived catalysts, respectively. These final values were very similar to those of the $Fe_3(CO)_{12}/C$ catalyst, and these changes are not due to variations in conversion or to thermodynamic effects caused by differences in temperature (*55*).

The presence of K clearly complicates any simple model, and the effect of K on the chemistry of the Fe–Mn system is presently not known. The influence of K certainly appears to mimic that of Mn and may well override any role of the Mn oxides. It does seem, however, that the Mn can still influence the product spectrum by lowering the average molecular weight of the product yield. Stencel *et al.* have shown that K interacts preferentially with MnO in a coprecipitated Fe/Mn catalyst, reducing the direct interaction with Fe (*34*). The phases of Fe present in that study as well as the mobility of the Mn and Fe species were altered by the introduction of potassium; consequently, we do not know the state of the active phase(s) in these K–Fe–Mn/C catalysts at this time.

SUMMARY

We have shown in this study that highly dispersed, carbon-supported Fe–Mn catalysts can be prepared from stoichiometric Fe–Mn and K–Fe–Mn carbonyl clusters. These systems not only replicate the high selectivities to olefins from CO and H_2 reported by others for bulk Fe–Mn catalysts, but also restrict the hydrocarbon product to light olefins—essentially ethylene, propylene, and butene. In addition, higher activities per gram of iron are attained at atmospheric pressure than with bulk catalysts operated at 10–11 atm.

The highest selectivities to light olefins were obtained with cluster-derived catalysts with Fe/Mn ratios of 2, and the addition of a potassium atom to the cluster further enhanced both selectivity and activity. The catalysts with a Fe/Mn ratio of 2 derived from nitrate salts did not exhibit this behavior. Based on the Fe/Mn stoichiometry and recent studies in the literature, we attribute the activity and high selectivity of the unpromoted catalysts to a mixed-spinel structure with a stoichiometry near Fe_2MnO_4. However, the addition of a K atom to the $Fe_3(CO)_{12}$ cluster also induces a pronounced shift such that the hydrocarbons contain only olefins and methane, but more chain growth seems to occur. The KFe_2Mn/C catalysts activated at 473 K appear to give optimum performance. The capability to activate these cluster catalysts at low temperature facilities both high dispersion and formation of the spinel structure, which is stable under reaction conditions. Reduction at high temperatures gives behavior similar to Fe-only catalysts and indicates that phase separation into reduced Fe and MnO may occur under these conditions.

ACKNOWLEDGMENTS

This study was a collaborative effort between the departments of Chemistry and Chemical Engineering which was funded by NSF Grant CPE-8205937. One of us (J.J.V.) acknowledges SASOL for partial support.

REFERENCES

1. Kölbel, H., Ralek, M., and Tillmetz, K. D., *in* "13th Int. Soc. Energy Conv., Soc. of Automot. Engrs.," p. 482 (1978).
2. Schulze, J., *Chem. Ing. Tech.* **46,** 925 (1974).
3. Kölbel, H., and Ralek, M., *Catal. Rev. Sci. Eng.* **21,** 225 (1980).
4. Hu, Y. C., *Hydrocarbon Process.* **62,** (1983).
5. Arakawa, H., and Bell, A. T., *in* "ACS Meeting, Div. Fuel Chem.," paper 56, Houston, TX 1980.
6. McVicker, G. B., and Vannice, M. A., *J. Catal.* **63,** 25 (1980).
7. Storch, H. H., Golumbic, H., and Anderson, R. B., "The Fischer–Tropsch and Related Synthesis," p. 234. Wiley, New York, 1951.
8. Kitzelmann, D., Vielstich, W., and Ditrich, T., *Chem. Ing. Tech.* **49,** 463 (1977).
9. Bussemeier, B., Frohning, C. D., and Cornils, B., *Hydrocarbon Process.* **55,** 105 (1976).
10. Fischer, F., and Tropsch, H. "Gesammelte Abhandlungen zur Kenntris der Kohle," Vol. 10, p. 407. Bontraeger, Berlin, 1932.
11. Kitzelmann, D., and Vielstich, W., *in* "2nd Kolloquim Fischer–Tropsch Synthese, Jülich, West Germany, 1978."
12. van Dijk, W. L., Niemantsverdriet, J. W., van der Kraan, A. M., and van der Baan, H. S., *Appl. Catal.* **2,** 273 (1982).
13. Madon, R. J., and Shaw, H., *Catal. Rev. Sci. Eng.* **15,** 69 (1977).
14. Kölbel, H., and Tillmetz, D. K., Belgian Patent 837,628.
15. Ralek, M., *in* "2nd Kolloquim Fischer–Tropsch Synthese, Jülich, West Germany, 1978."
16. Vannice, M. A., Walker, P. J., Jr., Jung, H. J., Morena-Castilla, C., and Mahajan, O. P., *in* "Proceedings, 7th Intl. Cong. on Catal., Tokyo, 1980," p. 460. Elsevier, Amsterdam, 1981.
17. Jung, H. J., Walker, P. L., Jr., and Vannice, M. A., *J. Catal.* **75,** 416 (1982).
18. El Deen, A. Z., Jacobs, J., and Baerns, M., *ACS Symp. Ser.* **65,** 26 (1978).
19. Maiti, G. C., Malessa, R., and Baerns, M., *Appl. Catal.* **5,** 151 (1983).
20. Lohrengel, G., and Baerns, M., *Ber. Bunsen Ges. Phys. Chem.* **87,** 335 (1983).
21. Jaggi, N. K., Schwartz, L. H., Butt, J. B., Papp, H., and Baerns, M., *Appl. Catal.* **13,** 347 (1985).
22. Bub, G., Baerns, M., Bussemeier, B., and Frohning, C., *Chem. Eng. Sci.* **35,** 348 (1980).
23. Deckwer, W. D., Lehmann, H. J., Ralek, M., and Schmidt, B., *Chem. Ing. Tech.* **53,** 818 (1981).
24. Deckwer, W. D., and Serpemen, Y., *I&EC Process. Des. Dev.* **21,** 222 (1982).
25. Lehmann, H. J., Nguen-Ngoc, H., Deckwer, W. D., and Ralek, M., *Chem. Ing. Tech.* **54,** 52 (1982).
26. Podesta, W., Guntzer, W., and Ralek, M., *Chem. Ing. Tech.* **55,** 631 (1983).
27. Satterfield, C. N., and Stenger, H. G., *I&EC Process. Des. Dev.* **23,** 26 (1984).
28. Satterfield, C. N., and Huff, G. A., *J. Catal.* **85,** 370 (1984).
29. Schulz, H., and Gökcebay, H., *in* "9th Conf. on Catal. of Org. React., Charleston, SC, USA, April, 1982."
30. Schulz, H., *in* "5th Intl. Conf. on Het. Catal., Varna, Bulgaria, Oct. 3–4, 1983."
31. Benecke, W., Schulz, H., Feller, H. G., and Ralek, M., *in* "Proceedings, 8th Intl. Cong. on Catal.," Vol. 4, p. 219. Dechema, Frankfurt, 1985.
32. Jensen, K. B., and Massoth, F. E., *J. Catal.* **92,** 98 (1985).
33. Jensen, K. B., and Massoth, F. E., *J. Catal.* **92,** 109 (1985).
34. Stencel, J. M., Diehl, J. R., Anderson, R. A., Zarochak, M. F., and Pennline, M. F., *Appl. Catal.*, in press.
35. Barrault, J., Forquy, Y. C., and Perrichon, V., *Appl. Catal.* **5,** 119 (1983).
36. Barrault, J., Renard, C., Yu, L. T., and Gal, J., *in* "Proceedings, 8th Intl. Cong. on Catal.," Vol. 2, p. 101. Dechema, Frankfurt, 1985.
37. Barrault, J., and Renard, C., *Appl. Catal.* **14,** 133 (1985).
38. Bruce, L., Hope, G., and Turney, T. W., *React. Kinet. Catal. Lett.* **20,** 175, (1982).
39. Kuznetsov, V. L., Danilyuk, H. F., Kolosova, I. E., and Yermakov, Y. I., *React. Kinet. Catal. Lett.* **21,** 249 (1982).
40. Anderson, J. R., and Mainwaring, D. E., *J. Catal.* **35,** 162 (1974).
41. Guczi, L., Schay, Z., Lazar, K., Vizi, A., and Marko, L., *Surf. Sci.* **106,** 516 (1981).
42. Kaminsky, M., Yoon, K. J., Geoffroy, G. L., and Vannice, M. A., *J. Catal.* **91,** 338 (1985).
43. Schubert, E. H., and Scheline, R. K., *Z. Naturforsch. B* **20,** 1306 (1965).
44. Ruff, J. K., *Inorg. Chem.* **7,** 1818 (1968).
45. Hodali, H. A., Arcus, C., and Schriver, D. F., *Inorg. Synth.* **20,** 218 (1980).
46. Schriver, D. F., "The Manipulation of Air Sensitive Compounds." McGraw–Hill, New York, 1969.
47. Amelse, J. A., Schwartz, L. H., and Butt, J. B., *J. Catal.* **72,** 95 (1981).
48. Jung, H. J., Vannice, M. A., Mulay, L. N., Stanfield, R. M., and Delgass, W. N., *J. Catal.* **76,** 208 (1982).
49. Vannice, M. A., *J. Catal.* **37,** 449 (1975).
50. Phillips, J., Clausen, B., and Dumesic, J. A., *J. Phys. Chem.* **84,** 1814 (1980).
51. Phillips, J., and Dumesic, J. A., *Appl. Surf. Sci.* **7,** 215 (1981).

52. Vannice, M. A., *in* "Catalysis—Science & Technology" (J. R. Anderson and M. Boudart, Eds.), Vol. 3, p. 140. Springer-Verlag, New York/Berlin, 1982.
53. Chen, A., Kaminsky, M., Geoffroy, G. L., and Vannice, M. A., *J. Phys. Chem.* **90,** 4810 (1986).
54. Storch, H. H., Golumbic, H., and Anderson, R. B., "The Fischer–Tropsch and Related Syntheses," p. 225. Wiley, New York, 1951.
55. Venter, J. J., Kaminsky, M., Geoffroy, G. L., and Vannice, M. A., *J. Catal.* **103,** 450 (1987).
56. Kölbel, H., and Haubold, H., *Ber. Bunsen Ges. Phys. Chem.* **65,** 421 (1961).
57. Kölbel, H., and Rohberg, H., *Ber. Bunsen Ges. Phys. Chem.* **75,** 1100 (1971).
58. Dry, M. E., Shingles, T., Boshoff, L. J., and Oosthuizen, G. J., *J. Catal.* **15,** 190 (1969).
59. Vannice, M. A., *Cat. Rev. Sci. Eng.* **14,** 153 (1976).
60. Emmett, P. H., and Brunauer, S., *J. Amer. Chem. Soc.* **59,** 319 (1937).
61. Topsoe, H., Topsoe, N., and Bohlbro, H., *in* "Proceedings, 7th Intl. Cong. Catal., Tokyo," p. 247. Elsevier, Amsterdam 1981.
62. Weatherbee, G. D., Rankin, J. L., and Bartholomew, C. H., *Appl. Catal.* **11,** 73 (1984).
63. Yoon, K. J., Walker, P. L., Jr., Mulay, L. N., and Vannice, M. A., *I&EC Prod. Res. Dev.* **22,** 519 (1983).
64. Hayward, D. O., and Trapnell, B. M. W., "Chemisorption," 2nd ed. Butterworths, Washington, 1964.
65. Boudart, M., Delbouille, A., Dumesic, J. A., Khammouma, S., and Topsoe, H., *J. Catal.* **37,** 486 (1975).
66. Kobayashi, M., and Shirasaki, T., *J. Catal.* **28,** 289 (1973).
67. Guerra, C. R., and Schulman, J. A., *Surf. Sci.* **7,** 229 (1967).
68. Yates, D. J. C., Murrell, L. L., and Prestridge, E. B., *J. Catal.* **57,** 41 (1979).
69. Bartholomew, C. H., and Pannell, R. B., *J. Catal.* **65,** 390 (1980).
70. Podgurski, H. H., Kummer, J. T., Dewitt, T. W., and Emmett, P. H., *J. Amer. Chem. Soc.* **72,** 5382 (1950).
71. Ford, R. R., *in* "Advances in Catalysis" (D. D. Eley, P. W. Selwood, and P. W. Weisz, Eds.), Vol. 21, p. 51. Academic Press, Orlando, FL, 1970.
72. Taylor, H. S., and Williamson, A. T., *J. Amer. Chem. Soc.* **53,** 2168 (1931).
73. Greenhalgh, E., Hayward, D. O., and Trapnell, B. M. W., *J. Phys. Chem.* **61,** 1254 (1957).
74. Bickley, R. I., Roberts, M. W., and Storey, W. C., *J. Chem. Soc. Inorg. Phys. Theor.*, p. 2774 (1971).
75. Blanchard, F., Reymond, J. P., Pommier, B., and Teichner, S. J., *J. Mol. Catal.* **17,** 171 (1982).
76. Anderson, R. B., *in* "Catalysis" (P. H. Emmett, Ed.), Vol. 4, p. 412. Reinhold, New York, 1956.
77. Raupp, G. B., and Delgass, W. N., *J. Catal.* **58,** 361 (1979).
78. Phillips, J., and Dumesic, J. A., *Appl. Catal.* **9,** 1 (1984).
79. Derouane, E. G., Baker, R. T. K., Dumesic, J. A., and Sherwood, R. D., *J. Catal.* **69,** 101 (1981).
80. Amelse, J. A., Butt, J. B., and Schwartz, L. H., *J. Phys. Chem.* **83,** 558 (1978).
81. Schaferstahl, H., *Angew. Chem. Int. Ed. Engl.* **19,** 729 (1980).
82. Niemantsverdriet, J. W., van der Kraan, A. M., van Dijk, W. L., and van der Baan, H. S., *J. Phys. Chem.* **84,** 3363 (1980).
83. Venter, J. J., M.S. thesis. The Pennsylvania State University, 1985.
84. Maiti, G. C., Malessa, R., Löchner, U., Papp, H., and Baerns, M., *Appl. Catal.* **16,** 215 (1985).
85. Bonzel, H. P., and Krebs, H. J., *Surf. Sci.* **91,** 449 (1980).
86. Bonzel, H. P., and Krebs, H. J., *in* "ACS Meeting, Houston, TX 1980. Div. Fuel Chem.," paper 53.
87. Bonzel, H. P., and Krebs, H. J., *Surf. Sci.* **109,** L527 (1981).
88. Bonzel, H. P., Krebs, H. J., and Schwarting, W., *Chem. Phys. Lett.* **72,** 165 (1980).
89. Bianchi, D., Tau, L. M., Borchar, S., and Bennett, C. O., *J. Catal.* **84,** 358 (1983).